Effects of Fractional Order and Variable Thermal Conductivity on Decaying-Heat Rotating Hydro-Semiconductor Medium

Kh. Lotfy[1], Ibrahim S. Elshazly[2], Borhen Halouani [3], and Saurav Sharma[4]
[1]*Department of Mathematics, Faculty of Science, P.O. Box 44519, Zagazig University, Zagazig, Egypt*
[2]*Department of Basic Sciences, Common First Year, King Saud University, Riyadh 11451, Saudi Arabia.*
[3]*Department of Mathematics, College of Science, King Saud University, P.O. Box 2455, Riyadh 11451, Saudi Arabia.*
[4]*University of Houston Cullen College of Engineering, 7900 Cambridge Street, #7-2G, Houston, Texas-77054, USA*
E-mail: khlotfy_1@yahoo.com; iali2.c@ksu.edu.sa; halouani@ksu.edu.sa; sauravkuk@gmail.com;

Abstract

This study investigates the combined effects of fractional order heat conduction and variable thermal conductivity on the propagation of thermal, acoustic, and optical waves in a rotating hydro-semiconductor medium. The novelty of this work lies in incorporating both fractional heat transfer theory and variable thermal conductivity within a hydrodynamic semiconductor model subjected to rotational effects, which has not been thoroughly explored in previous studies. The governing equations are formulated based on photo-thermoelasticity and fractional calculus, introducing a fractional heat conduction model to account for nonlocal and memory-dependent thermal responses. The normal mode analysis technique is applied. Numerical solutions are obtained and graphically represented to analyze the influence of fractional order parameters, variable thermal conductivity, and rotational effects. The results highlight significant deviations in wave propagation behavior when fractional heat transfer and thermal conductivity variations are included compared to classical heat conduction models.

Keywords: Fractional; Rotation; Thermal conductivity; Hydrodynamic; Semiconductor; Photoacoustic.

Nomenclature

λ, μ	Lame's parameters.
$\delta_n = (3\lambda + 2\mu) d_n$	Deformation potential coefficient.
T	Absolute temperature.
T_0	Reference temperature.
$\gamma = (3\lambda + 2\mu)\alpha_s$	The thermal expansion of volume.
α_s	The thermal expansion coefficient of semiconductor grains
ρ_s	Density of semiconductor grains
ρ_w	Density of pore water.
ρ	The density of the medium.
d_n	The electronic deformation coefficient
C_e	Specific heat of the medium.
K_0	Constant thermal conductivity.
D_E	The carrier diffusion coefficient.
τ	Lifetime.
t	Time variable
E_g	The energy gaps.
u_i	Displacement vector
N	Carrier concentration (density)
m	Volumetric heat capacity of medium
n_o	Porosity
τ_0	Thermal memory
P	Excess pore water pressure
α_w	Thermal expansion coefficient of pore water
g	Gravity
σ_{ij}	The stress tensor
C_w	Heat capacity of pore water
C_s	Heat capacity of semiconductor grains

k_d	Coefficient of permeability
P	Excess pore water pressure
e	Cubical dilatation
d_n	The coefficient of electronic deformation

1. Introduction

The interaction of thermal, mechanical, and optical fields in semiconductor materials has attracted increasing interest due to their wide-ranging applications in advanced optoelectronic devices, nanotechnology, and energy-efficient systems. These interactions are particularly crucial in hydro-semiconductors, which are characterized by their ability to exhibit coupled hydrodynamic and semiconductor behavior under thermal and mechanical excitation. The focus of this problem is on the intricate coupling of fractional order heat conduction, variable thermal conductivity, and rotational effects within hydro-semiconductors, where thermal, acoustic, and optical waves propagate under complex physical conditions. This work aims to address the growing need for a deeper understanding of such synergetic field interactions, which are pivotal for designing high-performance semiconductor-based technologies. The combined effects of fractional heat transfer theory and variable thermal conductivity in hydro-semiconductors have yet to be thoroughly explored, particularly under rotational fields. These factors profoundly influence the propagation characteristics of thermal and mechanical waves, especially in modern semiconductor applications where nonlocal effects, memory-dependent behavior, and spatial variations in conductivity are prominent. By incorporating photo-thermelasticity theory, this study examines the impact of these effects and provides a comparative analysis with classical heat conduction models.

Thermoelasticity is a classical theory that studies the coupled behavior of thermal and elastic fields in a solid medium. The foundations of thermoelasticity were established by Duhamel and Neumann, who demonstrated that temperature variations in an elastic material induce stress and deformation [1]. Over time, this theory evolved to include generalized thermoelasticity models such as the Lord-Shulman (LS) [2] and Green-Lindsay (GL) [3] models, which incorporate finite wave speeds for heat transfer, addressing the limitations of classical Fourier's law. The coupled thermoelasticity framework allows for the simultaneous treatment of thermal and mechanical fields, which is essential for understanding the wave propagation characteristics in materials subjected to dynamic thermal loads [4-6]. In recent years, the development of nonlocal thermoelasticity and fractional order heat theories has further expanded the applicability of thermoelasticity to nanoscale systems and materials with memory-dependent effects. Such advancements are particularly relevant to semiconductors, where thermal, optical, and mechanical fields interact at microscopic scales [7-10]. The inclusion of rotational effects introduces another layer of complexity to the analysis of hydro-semiconductors. Rotation induces Coriolis and centrifugal forces, which alter the propagation paths and speeds of thermal, acoustic, and optical waves. These rotational effects are particularly significant in rotating semiconductor devices, such as gyroscopes and sensors, where precision wave propagation is essential [11-14]. In hydro-semiconductors, the rotational field interacts with the hydrodynamic flow of charge carriers, leading to anisotropy in the wave propagation characteristics. The combined effects of rotation, fractional heat conduction, and variable thermal conductivity create a highly dynamic environment where thermal, mechanical, and optical waves exhibit unique behaviors. Understanding these effects is critical for optimizing the performance of semiconductor-based devices subjected to rotational motion [15-17].

Semiconductors are materials whose electrical conductivity can be precisely controlled, making them essential components in electronic and photonic devices [18]. The study of thermoelasticity in semiconductors becomes more complex when optical and thermal fields are introduced, leading to the development of photo-thermoelasticity theory [19, 20]. This theory describes the simultaneous interaction of optical (photon-induced), thermal, and elastic fields, providing a comprehensive framework for analyzing wave propagation in semiconductors [21]. In semiconductor materials, photon excitation causes temperature changes, which in turn generate stress and deformation [22]. The photo-thermoelastic effects are particularly significant in laser-excited systems, where intense thermal and optical loads influence the mechanical stability and wave propagation properties of the medium [23, 24]. The coupling of photo-thermoelasticity with hydrodynamic behavior further extends the applicability of this theory to modern semiconductor systems [25, 26].

The classical Fourier heat conduction model assumes an instantaneous response to thermal disturbances, which is unrealistic for systems with memory-dependent and nonlocal effects [27]. To address this limitation, fractional-order heat conduction theories have been developed. These models incorporate fractional calculus to describe the thermal diffusion process, allowing for the inclusion of memory and nonlocal behaviors. In semiconductors, fractional heat conduction plays a critical role in capturing the behavior of thermal waves at nano-scales and under short pulse heating conditions [28]. Fractional models are capable of describing sub-diffusive and super-diffusive thermal responses, which are essential for accurate thermal management in semiconductor devices. By combining fractional heat theories with photo-thermoelasticity, we can gain deeper insights into the propagation of coupled thermal and mechanical waves in semiconductor media [29].

Hydro-semiconductors are a special class of materials that exhibit both hydrodynamic and semiconductor behaviors [30-33]. In these materials, the flow of charge carriers (electron-hole plasma) behaves like a fluid, leading to significant interactions with thermal and mechanical fields [34-36]. The hydrodynamic nature of the charge carriers introduces viscous and inertial effects, which influence wave propagation in ways not observed in classical semiconductors [37-39]. Hydro-semiconductors are particularly relevant in high-frequency and high-power applications, where the coupled thermal, optical, and mechanical effects must be carefully managed [40-42]. By incorporating hydrodynamic models with photo-thermoelasticity, we can analyze the propagation of waves under dynamic thermal and mechanical loads, providing insights into the behavior of these advanced materials [43-45].

Thermal conductivity in semiconductors is not always constant and can vary with temperature, carrier density, and spatial position. In many real-world applications, such as high-power electronic devices and thermoelectric systems, thermal conductivity variations play a significant role in wave propagation behavior [46, 47]. This variability introduces additional complexity to the coupled thermal-mechanical analysis of semiconductors. Materials with temperature-dependent thermal conductivity exhibit nonlinear thermal responses, where the thermal wave speed and amplitude are influenced by the temperature gradient [48]. In hydro-semiconductors, where the hydrodynamic flow of charge carriers interacts with thermal fields, variable thermal conductivity further modulates the propagation characteristics of thermal, acoustic, and optical waves [49, 50].

This study addresses a significant gap in the literature by analyzing the combined effects of fractional order heat conduction, variable thermal conductivity, and rotational fields in hydro-semiconductor materials. These factors play a crucial role in the propagation of thermal, acoustic, and optical waves, particularly in modern high-performance semiconductor applications. The novelty of this work lies in its comprehensive approach, which incorporates fractional heat theories, photo-thermoelasticity, and hydrodynamic models to study the behavior of rotating semiconductor systems. The results presented in this study provide valuable insights into the interactions between thermal, mechanical, and optical fields, offering a deeper understanding of wave propagation in complex semiconductor environments. Graphical comparisons will illustrate the impact of fractional parameters, thermal conductivity variations, and rotational effects, highlighting the importance of these factors in wave propagation analysis. This work lays the foundation for future research on advanced semiconductor materials and their applications in optoelectronics, thermoelectric systems, and micro-electromechanical devices.

2. Mathematical model and basic equations

The study employs a hydro-photo-thermoelasticity framework, which considers photo-generated carrier interactions, thermal expansion, and mechanical stress. The governing equations are derived based on the fundamentals of poro-thermoelasticity theory, with suitable modifications to integrate both rotational dynamics and variable thermal conductivity. This approach enables a comprehensive understanding of wave behavior in rotating hydro-semiconductors, highlighting the combined influence of thermal, optical, and mechanical fields. Rotation introduces Coriolis $2\underline{\Omega} \times \dot{\underline{u}}$ and centrifugal forces $\underline{\Omega} \times (\underline{\Omega} \times \underline{u})$, where Ω represents the uniform angular velocity $(\underline{\Omega} = \Omega \hat{n})$ and $\hat{n}$ is the unit vector aligned with the rotation axis. The system's behavior is governed by the intricate interplay between thermal conduction, fluid motion, elastic deformations, and optical fields. Thermal conductivity effects, along with fractional heat conduction, are incorporated to account for scale-dependent responses and memory-driven thermal dynamics within the material. To obtain the main equations, we combine the laws of conservation of momentum, energy, and mass with constitutive relations for the fractional thermal behavior. This approach enables a comprehensive understanding of wave behavior in rotating hydro-semiconductors, highlighting the combined influence of thermal, optical, and mechanical fields.

(i) Charge Carrier Density N or plasma (Photo-thermal effects):

In semiconductor materials, the interaction of light with the medium generates photo-induced charge carriers, such as electrons and holes, leading to a change in the charge carrier density. This phenomenon, known as the photo-thermal effect, plays a significant role in the thermal and mechanical response of the medium due to the coupling between optical excitation, thermal conduction, and elastic deformations [30, 41, and 43].

$$\frac{\partial N}{\partial t} = D_E \nabla^2 N - \frac{N}{\tau} + \kappa T \,. \tag{1}$$

Here κ is the thermal activation coupling coefficient.

(ii) Equation of Motion with Rotation

The Equation of Motion with Rotation describes the dynamic behavior of a medium under the influence of rotational effects, where the inclusion of Coriolis and centrifugal forces modifies the motion of the system, leading to anisotropic wave propagation and altered mechanical responses [36, 44]:

$$\begin{aligned}(\lambda+\mu)\nabla(\nabla\cdot\vec{u})+\mu\nabla^{2}\vec{u}-\nabla P-\gamma\nabla T-\delta_{n}\nabla N = \\ (\underline{\ddot{u}}+\underline{\Omega}\,\mathrm{x}(\underline{\Omega}\,\mathrm{x}\underline{u})+2\underline{\Omega}\,\mathrm{x}\ \underline{\dot{u}})\end{aligned}. \tag{2}$$

Where $\varepsilon^{2}=\sqrt{ae_{0}/l}$ denotes the nonlocal parameter, l represents the external length scale, a expresses the internal length scale, and e_0 is the non-dimensional material property coefficient

(iii) The fractional heat equation

The fractional heat equation generalizes the classical heat conduction model by incorporating fractional derivatives of order α (α represents the parameter of fractional), which account for memory effects, providing a more accurate description of thermal behavior in materials with variable thermal conductivity [31, 36, 50]:

$$\nabla.(K\nabla T)-(1+\tau_{0}^{\alpha}\frac{\partial^{\alpha}}{\partial t^{\alpha}})\left(m\frac{\partial T}{\partial t}-\gamma T_{o}\frac{\partial e}{\partial t}\right)+\frac{E_{g}}{\tau}N=0. \tag{3}$$

Where $\frac{\partial^{\alpha}}{\partial t^{\alpha}}$ expresses the α -order fractional derivative (weak diffusion appears when $0<\alpha<1$, $\alpha=1$ gives the strong diffusion, super-diffusion appears when $0<\alpha<2$ and ballistic diffusion is obtained when $\alpha=2$) that can be applied to any function $n(t)$, yields [46]:

$$\lim_{\alpha\to1}\frac{d^{\alpha}}{dt^{\alpha}}n(t)=n'(t). \tag{4}$$

(iv) Fluid Flow Equation:

The fluid flow equation for a poro-semiconductor medium describes the movement of charge carriers as a fluid, considering the effects of porosity, pressure gradients, and interactions with thermal and mechanical fields, which are essential for analyzing coupled wave propagation [38-40]:

$$b_w(\alpha_w \frac{\partial T}{\partial t} - \frac{\partial e}{\partial t}) - \rho_w \frac{\partial^2 e}{\partial t^2} + \nabla^2 P = 0\,, \tag{5}$$

where $m = n_0 \rho_w C_w + (1-n_o)\rho_s C_s$ and $b_w = \dfrac{g\rho_w}{k_d}$.

(v) The constitutive relations are [32, 36]:

$$\sigma_{iI} = \lambda u_{r},_{r}\,\delta_{iI} + \mu u_{I,i} + \mu u_{i,I} - (P + \gamma T - \delta_n N)\delta_{iI}\,. \tag{6}$$

In many semiconductor materials, the thermal conductivity is not constant but varies with temperature, carrier density, or other factors, influencing heat distribution within the medium. Variable thermal conductivity $K(T)$ introduces additional complexity to thermal wave propagation, as the material's ability to conduct heat becomes dependent on the local conditions, leading to non-linear temperature gradients and altering the wave behavior, the linear dependent temperature form of thermal conductivity with negative small constant K_1, is:

$$K(T) = K_0(1 + K_1 T)\,, \tag{7}$$

The Kirchhoff transformation is a mathematical technique used to simplify heat conduction problems, particularly when dealing with varying material properties such as temperature-dependent thermal conductivity. By transforming the temperature field into a new coordinate system, the Kirchhoff transformation linearizes the governing equations, making it easier to solve for temperature distributions and analyze thermal wave propagation in media with spatially varying thermal properties.

$$\tilde{T}=\frac{1}{K_0}\int_0^T K(\chi)d\chi . \tag{8}$$

According to the linear form of thermal conductivity, yields:

$$K_0\tilde{T}_{,i}=K(T)T_{,i} \Rightarrow K_0\tilde{T}_{,ii}=(K(T)T_{,i})_{,i},\ K_0\dot{\tilde{T}}=K\dot{T} . \tag{9}$$

When the non-linear terms are ignored equation (8) can be rewritten as:

$$K_0\tilde{T}_{,ii}=K_{,i}T_{,i}+KT_{,ii}=K_0(1+K_1T)_{,i}T_{,i}+KT_{,ii}=K_0K_1(T_{,i})^2+KT_{,ii}=KT_{,ii} . \tag{10}$$

Studying the problem in a 2D hydro-semiconductor medium (in the *xz*-plane) involves analyzing the complex interactions between thermal, acoustic, and optical waves within a material subjected to various physical fields. In this context, the displacement field in 2D takes the form of a vector function $\vec{u}=(u,0,w)\ ;u=u(x,z,t)\ ,w=w(x,z,t),e=\frac{\partial u}{\partial x}+\frac{\partial w}{\partial z}$, which describes the deformation of the medium at any given point in space and time. This displacement field incorporates the effects of thermal expansion, mechanical stress, and photo-induced carrier generation, all of which contribute to the material's overall dynamic behavior. The governing equations for such a system are derived from the principles of hydro-photo-thermoelasticity, considering the two-dimensional nature of the medium, and accounting for rotational, thermal, and mechanical influences. In this case the 2D main governing equations with variable thermal conductivity (equations (7)-(10)) take the following form:

$$(\lambda+\mu)\frac{\partial e}{\partial x}+\mu\left(\frac{\partial^2 u}{\partial x^2}+\frac{\partial^2 u}{\partial z^2}\right)-\frac{\partial P}{\partial x}-\gamma\frac{\partial \tilde{T}}{\partial x}-\delta_n\frac{\partial N}{\partial x}= \left(\frac{\partial^2 u}{\partial t^2}-\Omega^2 u+2\Omega\dot{w}\right), \tag{11}$$

$$(\lambda+\mu)\frac{\partial e}{\partial z}+\mu\left(\frac{\partial^2 w}{\partial x^2}+\frac{\partial^2 w}{\partial z^2}\right)-\frac{\partial P}{\partial z}-\gamma\frac{\partial \tilde{T}}{\partial z}-\delta_n\frac{\partial N}{\partial z}= \left(\frac{\partial^2 w}{\partial t^2}-\Omega^2 w-2\Omega\dot{u}\right), \tag{12}$$

$$\sigma_{xx}=(2\mu+\lambda)\frac{\partial u}{\partial x}+\lambda\frac{\partial w}{\partial z}-\gamma T-P+(3\lambda+2\mu)d_n N\,, \tag{13}$$

$$\sigma_{zz}=(2\mu+\lambda)\frac{\partial w}{\partial z}+\lambda\frac{\partial u}{\partial x}-\gamma T-P+(3\lambda+2\mu)d_n N\,. \tag{14}$$

To simplify the governing equations that can be reduced into dimensionless form, we introduce dimensionless variables by scaling the original variables with respect to their characteristic scales. By applying these scaling transformations, the equations are simplified, making them more manageable and revealing the key parameters that govern the system's behavior. This approach not only reduces the complexity of the problem but also allows for a clearer understanding of the dominant physical effects and their relative importance.

$$\left.\begin{aligned}&\bar{N}=\frac{\delta_n}{2\mu+\lambda}N,(\bar{x}_i,\bar{u}_i,\bar{\varepsilon})=C_0\xi(x_i,u_i,\varepsilon),\bar{t}=C_0^2\xi t,(\bar{\tau},\bar{\tau}_o)=C_0^2\xi(\tau,\tau_o),\\&\bar{T}=\frac{\gamma}{2\mu+\lambda}T,\quad \bar{\sigma}_{ij}=\frac{\sigma_{ij}}{\mu},\bar{P}=\frac{P}{2\mu+\lambda},\xi=\frac{m}{K_0},C_0^2=\frac{\lambda+2\mu}{\rho},\Omega'=\frac{\Omega}{C_0^2\xi},.\end{aligned}\right\}. \tag{15}$$

Using equation (15) and the transformation, yields [46]:

$$(\nabla^2-\varepsilon_1-\varepsilon_2\frac{\partial}{\partial t})N+\varepsilon_3\tilde{T}=0\,, \tag{16}$$

$$(\lambda+\mu)\frac{\partial e}{\partial x}+\mu\left(\frac{\partial^2 u}{\partial x^2}+\frac{\partial^2 u}{\partial z^2}\right)-\frac{\partial P}{\partial x}-\gamma\frac{\partial \tilde{T}}{\partial x}-\delta_n\frac{\partial N}{\partial x}=\rho\left(\frac{\partial^2 u}{\partial t^2}-\Omega^2 u+2\Omega\dot{w}\right), \tag{17}$$

$$(\lambda+\mu)\frac{\partial e}{\partial z}+\mu\left(\frac{\partial^2 w}{\partial x^2}+\frac{\partial^2 w}{\partial z^2}\right)-\frac{\partial P}{\partial z}-\gamma\frac{\partial \tilde{T}}{\partial z}-\delta_n\frac{\partial N}{\partial z}=\rho\left(\frac{\partial^2 w}{\partial t^2}-\Omega^2 w-2\Omega\dot{u}\right), \tag{18}$$

$$\left(\nabla^2-(\frac{\partial}{\partial t}+\tau_0^\alpha\frac{\partial^{\alpha+1}}{\partial t^{\alpha+1}})\right)\tilde{T}+\varepsilon_7 N+\varepsilon_8(\frac{\partial}{\partial t}+\tau_0^\alpha\frac{\partial^{\alpha+1}}{\partial t^{\alpha+1}})e=0\,, \tag{19}$$

$$\nabla^2 P = \varepsilon_4 \frac{\partial e}{\partial t} + \varepsilon_5 \frac{\partial \tilde{T}}{\partial t} + \varepsilon_6 \frac{\partial^2 e}{\partial t^2}, \tag{20}$$

$$\sigma_{xx} = 2\frac{\partial u}{\partial x} + \frac{\lambda}{\mu} e - B^2(\tilde{T} + P - N), \tag{21}$$

$$\sigma_{zz} = 2\frac{\partial w}{\partial z} + \frac{\lambda}{\mu} e - B^2(\tilde{T} + P - N), \tag{22}$$

here

$$\varepsilon_1 = \frac{1}{\tau D_E \xi C_0^2}, \quad \varepsilon_2 = \frac{1}{D_E \xi C_0^2}, \quad \varepsilon_3 = \frac{\kappa \delta_n}{D_E C_0^4 \gamma \xi^2}, \varepsilon_4 = \frac{b_w}{\lambda + 2\mu}, \varepsilon_5 = -\frac{b_w \alpha_w}{\rho \xi},$$
$$\varepsilon_6 = -\frac{\rho_w}{\rho}, B^2 = \frac{\lambda + 2\mu}{\mu}, \varepsilon_7 = \frac{\gamma E_g}{\tau m \delta_n}, \varepsilon_8 = \frac{\gamma^2 T_0}{m(\lambda + 2\mu)}, \nabla^2 = \frac{\partial^2}{\partial x^2} + \frac{\partial^2}{\partial z^2}.$$

By using these scalar potentials $\Pi(x, y, t)$ and $\psi(x, y, t)$, the displacement components can be written as the gradient of the irrotational potential and the curl of the solenoidal potential, thus decoupling the system into more manageable equations. This formulation helps in reducing the complexity of the problem, especially in media where rotational effects and fluid-structure interactions play significant roles. Specifically, the displacement components can be expressed as [47, 48]:

$$u = \frac{\partial \Pi}{\partial x} + \frac{\partial \psi}{\partial z} \text{ and } w = \frac{\partial \Pi}{\partial z} - \frac{\partial \psi}{\partial x}. \tag{23}$$

These relationships help decouple the system and make the analysis of wave propagation in such complex media more tractable. This approach greatly simplifies the equations of motion, especially when dealing with a rotational and poroelastic medium. In this case, the equation of motion (17) and (18) can be introduced in the following form:

$$\left(\nabla^2 + \Omega^2 - \frac{\partial^2}{\partial t^2}\right)\Pi - \left(P + \tilde{T} + N\right) + 2\Omega \frac{\partial \psi}{\partial t} = 0, \tag{24}$$

$$\left(\nabla^2 - B^2\left(\frac{\partial^2}{\partial t^2} - \Omega^2\right)\right)\psi - 2\Omega B^2 \frac{\partial \Pi}{\partial t} = 0\,. \tag{25}$$

3. Solution to the problem

The normal mode technique is a powerful analytical method used to solve complex wave propagation problems, particularly in systems with multiple coupled fields such as thermal, mechanical, and optical waves. In this approach, the solution is assumed to be a sum of harmonically oscillating functions, each corresponding to a specific frequency of oscillation. The normal mode technique simplifies the analysis of wave interactions in heterogeneous media, such as hydro-semiconductors, by allowing the separation of different wave components (e.g., thermal, acoustic, or optical) and their contributions to the overall response of the system [31, 38]:

$$[N, e, \Pi, \psi, P, T, \sigma_{ij}](x, y, t) = [N^*, e^*, \Pi^*, \psi^*, P^*, \tilde{T}^*, \sigma_{ij}^*](x)\mathrm{e}^{(\omega t + ibz)}, \tag{26}$$

where ω represents the frequency, b is the wave number for each mode, and $N^*, e^*, \Pi^*, \psi^*, P^*, \tilde{T}^*$ and σ_{ij}^* express the amplitude based on the axis x. Substituting these expressions into the governing equations leads to a set of coupled equations for each mode as:

$$(D^2 - \alpha_1)N^* + \varepsilon_3 \tilde{T}^* = 0\,, \tag{27}$$

$$(D^2 - \alpha_3)\tilde{T}^* + \varepsilon_7 N^* - \alpha_4(D^2 - b^2)\Pi^* = 0\,, \tag{28}$$

$$(D^2 - b^2)P^* + \alpha_5(D^2 - b^2)\Pi^* + \alpha_6 \tilde{T}^* = 0\,, \tag{29}$$

$$(D^2 - \alpha_2)\Pi^* - (P^* + \tilde{T}^* + N^*) - \alpha_7 \psi^* = 0\,, \tag{30}$$

$$(D^2 - \alpha_8)\psi^* - \alpha_9 \Pi^* = 0\,, \tag{31}$$

$$\sigma_{xx}^* = 2Du^* + \frac{\lambda}{\mu}e^* - B^2(\tilde{T}^* + P^* - N^*)\,, \tag{32}$$

$$\sigma^*_{zz} = 2ibw^* + \frac{\lambda}{\mu} e^* - B^2(\tilde{T}^* + P^* - N^*)\,, \tag{33}$$

where $\frac{d}{dx} = D, \alpha_1 = b^2 + \varepsilon_1 + \omega\varepsilon_2, \alpha_2 = b^2 - \Omega^2 - \omega^2, \alpha_3 = b^2 + \omega(1 + \tau_0^\alpha \omega^\alpha)$,

$\alpha_4 = \varepsilon_8\omega(1 + \tau_0^\alpha \omega^\alpha), \alpha_5 = \omega(\varepsilon_4 + \omega\varepsilon_6), \alpha_6 = i\omega\varepsilon_5, \alpha_7 = 2\omega\Omega, \alpha_9 = 2B^2\Omega\omega,$

$\alpha_8 = b^2 - B^2(\omega^2 - \Omega^2)$.

The elimination technique for $N^*, e^*, \Pi^*, \psi^*, P^*, \tilde{T}^*$ and σ^*_{ij} that helps to simplify complex coupled systems by reducing the number of variables:

$$(D^8 - E_1D^6 + E_2D^4 - E_3D^2 + E_4)\{\tilde{T}^*, N^*, \Pi^*, \psi^*, P^*\}(x) = 0\,. \tag{34}$$

Here

$$E_1 = \left(\beta_3A_2 + A_3 + A_4\right)A_9^{-1}, \tag{35}$$

$$E_2 = \left(\beta_1A_{11} - \alpha_7\alpha_9A_7 + \alpha_4A_8 - \alpha_4\beta_3(\alpha_6 + \varepsilon_3) + \alpha_5A_{10}\right)A_9^{-1}, \tag{36}$$

$$E_3 = \left(\beta_1A_{12} - \alpha_7\alpha_9A_{13} + \alpha_4A_{14} - \alpha_5A_{15} + \alpha_4\alpha_6A_{16} + \varepsilon_3\alpha_4A_{17}\right)A_9^{-1}, \tag{37}$$

$$E_4 = \left(A_1A_{18} + \alpha_4\alpha_8b^2(\alpha_4 - \varepsilon_4)\right)A_9^{-1}, \tag{38}$$

$A_1 = \alpha_1\alpha_3 - \varepsilon_3\varepsilon_7$, $A_2 = \alpha_5 + \alpha_4 + \beta_1A_5$, $A_3 = \alpha_7\alpha_9\varepsilon^2(\varepsilon^2A_5 + 2\beta_2)$, $A_4 = \beta_1(\alpha_8 + \alpha_2\beta_3)$,

$A_5 = \alpha_1 + \alpha_3$, $A_6 = \alpha_2\alpha_8$, $A_{11} = \beta_3A_1 + A_4A_5 + A_6$, $A_7 = \varepsilon^2(\varepsilon^2A_1 + 2\beta_2A_5 - \beta_2^2)$,

$A_8 = \beta_3(b^2 + \alpha_1) + \alpha_8$, $A_9 = \beta_1\beta_3 - \alpha_7\alpha_9\varepsilon^4$, $A_{10} = \beta_3A_5 + \alpha_8$, $A_{16} = \beta_3\alpha_1 + \alpha_8$,

$A_{12} = A_1(\alpha_8 + \alpha_2\beta_3) + \alpha_2\alpha_8A_5$. $A_{13} = A_5\beta_2^2 + 2\varepsilon^2A_1\beta_2$, $A_{14} = \alpha_1b^2\beta_3 + \alpha_8(\alpha_1 + b^2)$,

$A_{15} = A_1\beta_3 - \alpha_8A_5$, $A_{17} = \beta_3b^2 + \alpha_8$, $A_{18} = \alpha_8(\alpha_2\beta_1 + \alpha_5) - \alpha_7\alpha_9\beta_2^2$.

To represent an ordinary differential equation (ODE), such as equation (32), in a factored form, the goal is to express it as a product of simpler terms, which can make it easier to solve or analyze. Here is a general approach to rewriting an ODE in a factored form:

$$\prod_{i=1}^{4}(D^2 - k_i^2)\left(\tilde{T}^*, N^*, \Pi^*, \psi^*, P^*\right)(x) = 0\,. \tag{39}$$

$k_n^2 (n=1,2,3,4)$ are the roots (chosen in positive and real) of the characteristic equation (39). The solution to the homogeneous equation (39) will take the form:

$$\left\{\tilde{T}^*, N^*, \Pi^*, \psi^*, P^*\right\}(x) = \sum_{n=1}^{4} M_n \left\{1, a^*, b^*, c^*, d^*\right\} e^{-k_n x}, \tag{40}$$

where

$$a_n^* = \frac{-\varepsilon_3}{k_n^2 - \alpha_1}, \quad b_n^* = \frac{k_n^4 - (\alpha_1 + \alpha_3)k_n^2 + A_1}{\alpha_4 (k_n^2 - \alpha_1)(k_n^2 - b^2)}, c_n^* = \frac{\alpha_9 (\varepsilon^2 k_n^2 - B_2)(k_n^4 - (\alpha_1 + \alpha_3)k_n^2 + A_1)}{\alpha_4 (k_n^2 - \alpha_1)(B_3 k_n^2 - \alpha_8)(k_n^2 - b^2)},$$

$$d_n^* = -\frac{\alpha_5 (k_n^4 - (\alpha_1 + \alpha_3)k_n^2 + A_1) + \alpha_4 \alpha_6 (k_n^2 - \alpha_1)}{\alpha_4 (k_n^2 - \alpha_1)(k_n^2 - b^2)}.$$

From the boundary conditions, M_n (are unknown coefficients) can be obtained. To express the 2D displacement components u and w in terms of a scalar potential Π and a vector potential ψ, we use the following standard decomposition in the context of a fractional-rotational and poroelastic semiconductor medium:

$$u^*(x) = D\Pi^* + ib\, \psi^* = \sum_{n=1}^{4} M_n (-k_n b^* + ibc^*) e^{-k_n x}, \tag{41}$$

$$w^* = ib\Pi^* + k_n \psi^* = \sum_{n=1}^{4} M_n (ibb^* + k_n c^*) e^{-k_n x}. \tag{42}$$

Assuming that equations (32) and (33) provide relationships between the strain and stress tensors, we can express the stress-strain relation in a reformulated form:

$$\sigma_{xx}^*(x) = \sum_{n=1}^{4} \left(\frac{2(k_n^2 b^* - ibk_n c^*) + \dfrac{\lambda}{\mu}(k_n^2 - b^2)b^* - B^2(1 + d^* - a^*)}{\alpha_8 - \varepsilon^2 k_n^2} \right) M_n e^{-k_n x}, \tag{43}$$

$$\sigma_{zz}^*(x) = \sum_{n=1}^{4} \left(\frac{2b(ik_n c^* - bb^*) - \dfrac{\lambda}{\mu}(k_n^2 + b^2)b^* - B^2(1 + d^* - a^*)}{\alpha_8 - \varepsilon^2 k_n^2} \right) M_n e^{-k_n x}. \tag{44}$$

4. Boundary conditions

In the context of wave propagation problems, the decay parameter often refers to how the amplitude of a wave decays or diminishes with distance. For boundary conditions involving the decay parameter, especially in problems related to wave propagation in elastic, poroelastic, or hydroelastic media, these conditions typically specify how the waves behave at the boundaries, especially as they extend to infinity or approach a boundary where their effect diminishes. To obtain the values of M_n, some boundary conditions at $x = 0$ involving a decay parameter for a hydro-semiconductor are introduced [42, 43]:

1) If the system involves waves propagating outward in a semi-infinite domain, the thermal boundary condition can be expressed in terms of a decay parameter. If thermal effects are present, a similar decay condition can be applied to the temperature field.

$$\tilde{T}^*(0, z, t) = T_0 \exp(-\lambda t) \,. \tag{45}$$

Where λ the decay parameter is associated with the rate of thermal diffusion. The decay parameter plays an important role in defining the boundary conditions for wave propagation problems in media with rotational, poroelastic, and photothermal effects. By introducing a decay factor (exponential), these boundary conditions help model the dissipation of wave amplitude, stress, strain, or energy at the boundary, allowing for more realistic solutions that consider damping.

2) In the context of hydroelastic media (e.g., in a hydro semiconductor medium or similar systems), the excess pore water pressure boundary condition is crucial for modeling the behavior of the fluid phase (e.g., water or another fluid) within the pores of the material. The excess pore pressure reflects the deviation of the pore pressure from its equilibrium value and can significantly affect wave

propagation, especially in porous materials. If the boundary is impermeable, meaning there is no flow of fluid through the boundary, the excess pore pressure at the boundary is either constant P_0 (is the prescribed excess pore pressure at the boundary):

$$P(0,z,t) = P_0 . \tag{46}$$

3) The **carrier density** boundary condition in a semiconductor or hydro-semiconductor medium governs the distribution of charge carriers (such as electrons or holes) at the material's surface or interface. This is a crucial factor in many semiconductor physics problems, especially when photothermal or photoelastic effects are considered, and it can influence the propagation of waves within the material. For a system with waves propagating in the semiconductor, the carrier density may decay as it moves away from a source or the material's boundary. This can happen, for instance, when the semiconductor is excited by a localized source, and the carrier density decreases with distance from the source. With equilibrium carrier concentration N_0 , this condition takes the form:

$$N^*(0,z,t) = N_0 \exp(-\lambda t) . \tag{47}$$

4) The boundary conditions for stress generally specify the mechanical behavior at the surface of the material or the interface with other materials (e.g., air). If the stress at the boundary is known and fixed (for example, from an external force or a uniform pressure applied on the surface), the boundary condition can specify the stress directly. This condition is common when a uniform load or pressure φ_1 is applied to the material:

$$\sigma_{xx}(0,z,t) = -\varphi_1 . \tag{48}$$

By applying boundary conditions (45)-(48) and using normal mode analysis, the problem is reduced to a system of equations for the spatial components of the fields.

$$\sum_{n=1}^{4} M_n = T_0 \exp(-\lambda t), \tag{49}$$

$$\sum_{n=1}^{4}\left(-\frac{\alpha_5(k_n^4-(\alpha_1+\alpha_3)k_n^2+A_1)+\alpha_4\alpha_6(k_n^2-\alpha_1)}{\alpha_4(k_n^2-\alpha_1)(k_n^2-b^2)}\right)M_n = P_0^*, \tag{50}$$

$$-\sum_{n=1}^{4}\frac{\varepsilon_3}{k_n^2-\alpha_1}M_n = N_0 \exp(-\lambda t)\ , \tag{51}$$

$$\sum_{n=1}^{4}\left(\frac{2b(ik_nc^*-bb^*)-\frac{\lambda}{\mu}(k_n^2+b^2)b^*-B^2(1+d^*-a^*)}{\alpha_8-\varepsilon^2k_n^2}\right)M_n = -\varphi_1^*. \tag{52}$$

These equations can then be solved to obtain the mode shapes and dispersion relations for the system, which describe how the fields propagate and interact under the influence of external forces, rotational fields, and other material effects

5. Validation

To assess the validity of the proposed model and its predictions related to wave propagation, thermal diffusion, and mechanical stress in hydro-semiconductors subjected to rotational effects, variable thermal conductivity and fractional-order derivatives, several key scenarios were considered.

5.1 The rotation effect

When the rotational angular parameter is disregarded ($\Omega = 0$), the study focuses on variable thermal conductivity the behavior of a fractional hydro-semiconductor medium. In this case, the motion equation is simplified as outlined in [44]:

$$(\lambda+\mu)\nabla(\nabla\cdot\vec{u})+\mu\nabla^2\vec{u}-\nabla P-\gamma\nabla\tilde{T}-\delta_n\nabla N=\underline{\ddot{u}}\ . \tag{53}$$

5.2 The variable thermal conductivity impacts

When the variable thermal conductivity is excluded ($K_1 = 0$ and $K = K_0$), the analysis is carried out for a fractional hydro-semiconductor medium with rotational effects. The resulting motion equations are derived as presented in [41]:

$$K\nabla^2 T - (1+\tau_0^\alpha \frac{\partial^\alpha}{\partial t^\alpha})\left(m\frac{\partial T}{\partial t} - \gamma T_o \frac{\partial e}{\partial t}\right) + \frac{E_g}{\tau} N = 0. \quad (54)$$

5.3The fractional parameter

The heat equation is an extension of the classical form, incorporating fractional derivatives to capture scale-dependent and memory effects. When the fractional derivative of order α is set to 1 ($\alpha = 1$), the heat equation reverts to its classical form as follows [43]:

$$\nabla.(K\nabla T) - (1+\tau_0 \frac{\partial}{\partial t})\left(m\frac{\partial T}{\partial t} - \gamma T_o \frac{\partial e}{\partial t}\right) + \frac{E_g}{\tau} N = 0. \quad (55)$$

5.4The photo-thermoelasticity theories

When the thermal relaxation time effect is ignored ($\tau_o = 0$), the equations reduce to classical coupled thermoelasticity theory (CD) [47]. On the other hand, when $\tau_o > 0$ is considered, the model predicts the Lord and Shulman (LS) model.

6. Numerical results and discussions

In this section, we present the numerical results and a thorough discussion of our study, which is based on the physical constants of poro-silicon (PSi) for performing the calculations. The computations are conducted using MATLAB to ensure precision in the modeling and analysis process. All parameters are expressed in SI units to maintain uniformity and standardization throughout the study. The following analysis provides a comprehensive review of the numerical solutions and their significance in the context of the poroelastic model. The physical constants specific to the PSi medium are listed in Table 1 [49, 50].

Unit	Symbol	Value	Unit	Symbol	Value
N/m^2	λ μ	3.64×10^{10} 5.46×10^{10}	N	p	100
kg/m^3	ρ_s	2.3×10^3	$1/cm^3$	N_0	9.65×10^9
K	T_0	800	kg/m^3	ρ_w	10^3
S	τ	5×10^{-5}	m/s	k_d	10^{-8}
m^3	d_n	-9×10^{-31}	$J/kg\,K$	C_w	4×10^3
m^2/s	D_E	2.5×10^{-3}	$^oC^{-1}$	α_w	2×10^{-4}
eV	E_g	1.11	$J/kg\,K$	C_s	6×10^2
K^{-1}	α_s	4.14×10^{-6}	$J/kg\,K$	C_e	695
$Wm^{-1}K^{-1}$	K	150	S	τ_o	0.0002
kg/m^3	ρ	2000	$\varphi_1^*=0.5$	$\theta_1=300\,K$	$n_0=0.4$
$\omega=\omega_0+i\xi$	$\omega_0=-2$	$\xi=0.001$	$i=\sqrt{-1}$	$t=0.02\,s$	$b=1$

Table 1: The physical constants of the PSi material

6.2. The influence of variable thermal conductivity

Figure 2 illustrates the impact of variable thermal conductivity K_1 on the propagation of primary physical fields (temperature, horizontal and vertical displacements, carrier density, normal stress, and excess pore water pressure) against the distance x for a fractional heat order of $\alpha=0.5$, under the influence of rotational fields and the decay parameter $\lambda=0.3$. Three cases are presented: $K_1=0$ (constant thermal conductivity), $K_1=-0.03$, and $K_1=-0.06$ (temperature-dependent thermal conductivity). Temperature Field T : The results show a sharp initial peak, followed by a gradual decay. With increasing thermal conductivity dependence ($K_1=-0.03$, and $K_1=-0.06$), the temperature decreases more rapidly, indicating enhanced thermal diffusion due to the temperature-dependent thermal conductivity, which accelerates heat dissipation.The oscillatory behavior of horizontal displacement diminishes with increased thermal conductivity variation. The amplitude reduces notably for higher K_1, reflecting the energy loss through enhanced thermal conduction, which suppresses the mechanical response. Similar to horizontal displacment, vertical displacement exhibits higher initial amplitudes for smaller K_1 and diminishes more rapidly as thermal conductivity becomes temperature-dependent. This demonstrates the coupled effect of thermal and mechanical fields, where temperature variations dampen the mechanical wave propagation. The carrier density decreases more steeply with increasing thermal conductivity dependence. This behavior indicates that the thermal effect accelerates the redistribution of photo-generated carriers, reducing their concentration over shorter distances. The stress field displays pronounced oscillations with smaller K_1 increases in magnitude ($K_1 = -0.06$), the oscillations are dampened, reflecting the influence of thermal diffusion on mechanical stress, where enhanced heat conduction mitigates stress accumulation. The pore pressure initially increases and then oscillates as the distance progresses. Higher thermal conductivity variation ($K_1 = -0.06$) amplifies the oscillations, indicating that thermal effects strongly influence fluid flow behavior within the porous medium. The results emphasize the significant role of variable thermal conductivity in the coupled photo-thermo-mechanical responses of hydro-semiconductor media. As thermal conductivity becomes more temperature-dependent, thermal diffusion increases, leading to faster dissipation of thermal energy, reduced mechanical wave amplitudes, and accelerated redistribution of carriers and fluid pressure. The rotational field and decay parameter further influence wave attenuation and propagation characteristics, highlighting the interplay between thermal, mechanical, and fluid fields in such complex media.

6.2. The impact of fractional-order parameter

Figure 2 demonstrates the effect of the fractional-order parameter α on the key dimensionless physical fields (temperature, displacements, carrier density, stress, and pore water pressure) in a hydro-semiconductor medium under rotational effects and variable thermal conductivity with a decay parameter. Three cases are considered: $\alpha = 0$ (classical derivative, CD), $\alpha = 0.5$ (fractional case, FR), and $\alpha = 1$ (local derivative, LS model). The temperature field reveals that the classical derivative ($\alpha = 0$) decays more rapidly compared to the fractional case and local derivative, indicating that fractional effects extend the influence of thermal diffusion over a larger spatial domain. The two displacement components show significant oscillations, with $\alpha = 0.5$ producing intermediate damping behavior, highlighting the fractional model's role in balancing local and nonlocal characteristics. Carrier density (middle-right) exhibits sharper peaks in the local case ($\alpha = 1$), while the fractional case smoothens the distribution. Stress, and excess pore water pressure display oscillatory behavior, with the fractional case providing a transition between highly damped ($\alpha = 0$) and less damped ($\alpha = 1$) responses. This analysis reveals that the fractional-order parameter significantly influences wave propagation, thermal diffusion, and mechanical responses, offering a versatile framework to capture both local and memory-dependent behaviors in hydro-semiconductor systems under rotational effects.

6.3 Impact decay parameter

Figure 4 illustrates the wave propagation of the primary physical fields against distance x for varying decay parameters under the combined effects of a rotational field and variable thermal conductivity $K_1 = -0.06$ with fractional heat order $\alpha = 0.5$. The results demonstrate that the decay parameter significantly influences the amplitude and attenuation of the wave profiles. For temperature and carrier density fields, increasing the decay parameter leads to more rapid attenuation as the distance increases, indicating stronger energy dissipation. The horizontal and vertical displacements exhibit oscillatory behavior, with the amplitude and wavelength varying based on the decay parameter, reflecting the influence of thermal and rotational effects on elastic deformation. Similarly, the normal stress and excess pore water pressure fields show more pronounced oscillations and slower attenuation for smaller decay parameters, while larger values accelerate the damping of oscillations. Physically, this suggests that higher decay parameters enhance energy dissipation and reduce wave propagation effects, while the rotational field and variable thermal conductivity modulate the interaction between thermal, mechanical, and elastic responses in the medium.

Conclusions

In this study, we investigated the propagation of thermal, mechanical, and carrier density waves in a hydro-semiconductor medium under the combined effects of a rotational field, fractional heat theory, and variable thermal conductivity. The results revealed significant insights into the influence of fractional-order parameters and thermal decay on wave behavior, including oscillations, and the distribution of physical fields such as temperature, displacements, stresses, and pore water pressure. Fractional heat order introduced a more generalized and realistic description of heat conduction, providing a smoother transition between classical and nonlocal thermal responses. Additionally, the variable thermal conductivity parameter played a critical role in controlling energy dissipation and wave propagation distance. The findings of this study have practical applications in several advanced technologies and industries. For example, in semiconductor manufacturing, understanding wave propagation under variable thermal conductivity aids in designing efficient thermal management systems for microelectronics and nano-devices. In geophysical engineering, the results apply to the analysis of subsurface thermal and mechanical behavior, such as heat and stress distribution in hydro-poroelastic materials subjected to rotational forces.

Declarations

Conflict of interest: The corresponding author states that there is no conflict of interest.

Acknowledgement: The authors would like to extend their sincere appreciation to Researchers Supporting Project number (RSPD2024R1112), King Saud University, Riyadh, Saudi Arabia.

Funding: The authors would like to extend their sincere appreciation to Researchers Supporting Project number (RSPD2024R1112), King Saud University, Riyadh, Saudi Arabia.

Author contributions: All authors have equally participated in the preparation of the manuscript during the implementation of ideas, findings results, and writing of the manuscript.

Data Availability: Current submission does not contain the pool data of the manuscript but the data used in the manuscript will be provided on request.

Use of AI tools declaration: The authors declare they have not used Artificial Intelligence (AI) tools in the creation of this article.

Ethical approval: Not applicable.

ORCID ID: Khaled Lotfy: https://orcid.org/0000-0001-9383-1361.

References

[1] M. A. Biot, Thermoclasticity and irreversible thermodynamics. J. Appl. Phys. 27, 240-253(1956).

[2] H. W. Lord and Y.Shulman, A generalized dynamical theory of thermolasticity, J. Mech. Phys. Solids. 15, 299-306 (1967).

[3] A. E. Green and K. A. Lindsay, Thermoelasticity, J. Elasticity. 2, 17 (1972).

[4] A. Green, and P. Naghdi, A reexamination of the basic results of themomechanics, Proceedings of the Royal Society of London A, 432, 171-194, (1991).

[5] A. Green, and P. Naghdi, On undamped heat waves in an elastic solid, Journal of Thermal Stresses, 15, 252-264, (1992).
[6] D.Y. Tzou, A unified field approach for heat conduction from macro to micro scales, ASME Journal of Heat Transfer, 117, 8-16, (1995).
[7] H.M. Youssef, Theory of two-temperature-generalized thermoelasticity, IMA Journal of Applied Mathematics, 71, 383-390, (2006).
[8] R.B. Hetnarski, and J. Ignaczak, Generalized thermoelasticity, Journal of Thermal Stresses, 22, 451-476, (1999).
[9] P. Lata and I. Kaur, A Study of Transversely Isotropic Thermoelastic Beam with Green-Naghdi Type-II and Type-III Theories of Thermoelasticity, Applications and Applied Mathematics, 14(1), Article No 17, (2019). https://digitalcommons.pvamu.edu/aam/vol14/iss1/17.
[10] Kh. Lotfy, Mode-I crack in a two-dimensional fibre-reinforced generalized thermoelastic problem, Chinese Physics B, 21(1), 014209, (2012).
[11] P. Ailawalia, and N. Singh, Effect of rotation in a generalized thermoelastic medium with hydrostatic initial stress subjected to ramp type heating and loading, Int. J. Thermophys, 30, 2078–2097, (2009).
[12] I. Abbas and R. Kumar, Response of thermal source in initially stressed generalized thermoelastic half-space with voids, J. Comput. Theoret. Nanosci, 11(6), 1472–1479, (2014).
[13] M. Bachher, N. Sarkr and A. Lahiri, Generalized thermoelastic infinite medium with voids subjected to an instantaneous heat source with fractional derivative heat transfer, Int. J. Mech. Sci., 89, 84–91, (2014).
[14] P. Ailawalia, M. Marin, Response of a semiconducting medium under photothermal theory due to moving load velocity, Waves in Random and Complex Media, 32(4), 1644–1653, (2020). https://doi.org/10.1080/17455030.2020.1831709.
[15] M. Marin, A. Öchsner, M. Bhatti, Some results in Moore-Gibson-Thompson thermoelasticity of dipolar bodies, (ZAMM) Zfur Angew. Math. Mech. 100(12), Art No. e202000090, (2020).
[16] Kh. Lotfy, and W. Hassan, Effect of Rotation for Two-Temperature Generalized Thermoelasticity of Two-Dimensional under Thermal Shock Problem, Mathematical Problems in Engineering, 13, 297274, (2013). https://doi.org/10.1155/2013/297274.
[17] S. Abo-Dahab, A. Abd-Alla, A. Alqarni, A two-dimensional problem with rotation and magnetic field in the context of four thermoelastic theories, Results in Physics, 7, 2742-2751, (2017).

[18] J. Gordon, R. Leite, R. Moore, S. Porto, J. Whinnery, Long-transient effects in lasers with inserted liquid samples. Bull Am Phys Soc., 119, 501–510, (1964).
[19] L. Kreuzer, Ultralow gas concentration infrared absorption spectroscopy. J Appl Phys., 42(7):2934–2943, (1971).
[20] Sh. El-Sapa, A. Almoneef, Kh. Lotfy, A. El-Bary, A. Saeed,Moore-Gibson-Thompson theory of a non-local excited semiconductor medium with stability studies, Alexandria Engineering Journal, 61(12), 11753-11764, (2022).https://doi.org/10.1016/j.aej.2022.05.036.
[21] S. Hosseini, C. Zhang, Plasma-affected photo-thermoelastic wave propagation in a semiconductor Love–Bishop nanorod using strain-gradient Moore–Gibson–Thompson theories, Thin-Walled Structures, 179, 109480, (2022).
[22] A. Abouelregal, H. Sedighi, S. Megahid, Photothermal-induced interactions in a semiconductor solid with a cylindrical gap due to laser pulse duration using a fractional MGT heat conduction model. Arch Appl Mech., 93, 2287–2305, (2023).
[23] J. Liu, M. Han, R. Wang, S. Xu, and X. Wang, Photothermal phenomenon: Extended ideas for thermophysical properties characterization, J. Appl. Phys. 131, 065107, doi: 10.1063/5.0082014, (2022).
[24] Kh. Lotfy, E. Elidy and R. Tantawi, Photothermal Excitation Process during Hyperbolic Two-Temperature Theory for Magneto-Thermo-Elastic Semiconducting Medium. Silicon 13, 2275–2288 (2021).
[25] Kh. Lotfy, A. El-Bary, E. Ismail, H. Atef, Analytical solution of a rotating semiconductor elastic medium due to a refined heat conduction equation with hydrostatic initial stress, Alexandria Engineering Journal, 59 (6), 4947-4958, (2020). https://doi.org/10.1016/j.aej.2020.09.012.
[26] Kh. Lotfy, A. El-Bary and A. El-Sharif, Ramp-type heating microtemperature for a rotator semiconducting material during photo-excited processes with magnetic field, Results in Physics, 19, 103338, (2020).
[27] S. Askar, A. Abouelregal, M. Marin, A. Foul, Photo-Thermoelasticity Heat Transfer Modeling with Fractional Differential Actuators for Stimulated Nano-Semiconductor Media. Symmetry 2023, 15, 656. https://doi.org/10.3390/sym15030656.
[28] K. Zakaria, M. Sirwah, A. Abouelregal, A. Rashid, Photo-Thermoelastic Model with Time-Fractional of Higher Order and Phase Lags for a Semiconductor Rotating Materials, Silicon 13, 573–585 (2021). https://doi.org/10.1007/s12633-020-00451-z.

[29] A. Zenkour, A. Abouelregal, Fractional Thermoelasticity Model of a 2D Problem of Mode-I Crack in a Fibre-Reinforced Thermal Environment, J. Appl. Comput. Mech., 5(2), 269-280, (2019).
[30] M. Adel, Kh. Lotfy, A. Yadav, E. Ibrahim, Orthotropic rotational semiconductor material with piezo-photothermal plasma waves with moisture plasma diffusion and laser pulse. Z Angew Math Mech. 2301004 (2024). https://doi.org/10.1002/zamm.202301004.
[31] H. Liu, F. Wang A novel semi-analytical meshless method for the thickness optimization of porous material distributed on sound barriers, Applied Mathematics Letters, 147, 108844, (2024).
[32] R. Kumar, and S. Devi, Thermomechanical intereactions in porous generalized thermoelastic material permeated with heat sources, Multidiscipline Modeling in Materials and Structures, 4, 237-254, (2008).
[33] H. Sherief, and E. Hussein, A mathematical model for short-time filtration in poroelastic media with thermal relaxation and two temperatures, Transport in Porous Media, 91,199-223, (2012).
[34] I. Abbas, and H. Youssef, Two-dimensional fractional order generalized thermoelastic porous material, Latin American Journal of Solids and Structures, 12,1415-1431, (2015).
[35] W. Wei, R. Zheng, G. Liu and H. Tao, Reflection and refraction of P wave at the interface between thermoelastic and porous thermoelastic medium, Transport in Porous Media, 113, 1-27, (2016).
[36] M. Schanz, Poroelastodynamics: linear models, analytical solutions, and numerical methods, Applied Mechanics Reviews, 62(3), 030803, (2009). Doi:10.1115/1.3090831
[37] M. Marin, A. Hobiny, and I.Abbas, Finite element analysis of nonlinear bioheat model in skin tissue due to external thermal sources, Mathematics, 9(13), Art. No. 1459, (2021).
[38] Y. Abousleiman and S. Ekbote, Solutions for the inclined borehole in a porothermoelastic transversely isotropic medium, Transactions of the ASME. E: Journal of Applied Mechanics, 72, 102-114, (2005).
[39] J. Booker, and C. Savvidou, Consolidation around a spherical heat source, International Journal of Solids and Structures, 20, 1079-1090, (1984).
[40] M. Biot, Variational Lagrangian-thermodynamics of non-isothermal finite strain mechanics of porous solids and thermomolecular diffusion, International Journal of Solids and Structures, 13, 579-597, (1977).

[41] C. Xiong, G. Ying and D. Yu, Normal Mode Analysis to a Poroelastic Half-Space Problem under Generalized Thermoelasticity, Lat. Am. j. solids struct., 14 (5), 930-949, (2017). https://doi.org/10.1590/1679-78253611.
[42] M. Marin, I. Abbas and R. Kumar, Relaxed Saint-Venant principle for thermoelastic micropolar diffusion, Struct. Eng. Mech., 51(4), 651-662, (2014).
[43] R. Kimmich, Strange kinetics, porous media, and NMR, J. Chem. Phys., 284, 243–285, (2002).
[44] H. Alshehri, Kh. Lotfy; A novel hydrodynamic semiconductor model under Hall current effect and laser pulsed excitation. Physics of Fluids, 36 (12), 122005, (2024). https://doi.org/10.1063/5.0241229.
[45] M. Raddadi, M. Alotaibi, A. El-Bary, Kh. Lotfy, A novel generalized photo-thermoelasticity model for hydro-poroelastic semiconductor medium. AIP Advances, 14 (12): 125104, (2024).
[46] H. Youssef, and A. El-Bary, Thermal shock problem of a generalized thermoelastic layered composite material with variable thermal conductivity. Mathematical Problems in Engineering, 2006, 87940, 1–14, (2006). doi: 10.1155/mpe/2006/87940
[47] Sh. El-Sapa, Kh. Lotfy, E. Elidy, A. El-Bary and R. Tantawi, Photothermal Excitation Process in Semiconductor Materials under the Effect Moisture Diffusivity, Silicon, 15, 4171–4182, (2023).
[48] M. Yasein, N. Mabrouk, Kh. Lotfy and A.EL-Bary, The influence of variable thermal conductivity of semiconductor elastic medium during photothermal excitation subjected to thermal ramp type. Results in Physics, 15, 102766, (2019).
[49] I. Abbas, A. Hobiny, M. Marin, Photo-thermal interactions in a semi-conductor material with cylindrical cavities and variable thermal conductivity. Journal of Taibah University for Science, 14(1), 1369–1376, (2020). doi: 10.1080/16583655.2020. 1824465
[50] A. Sharma, J. Sharma, and Y. Sharma, Modeling reflection and transmission of acoustic waves at a semiconductor: fluid interface, Adv. Acoust. Vib., 2012, 637912, (2012).

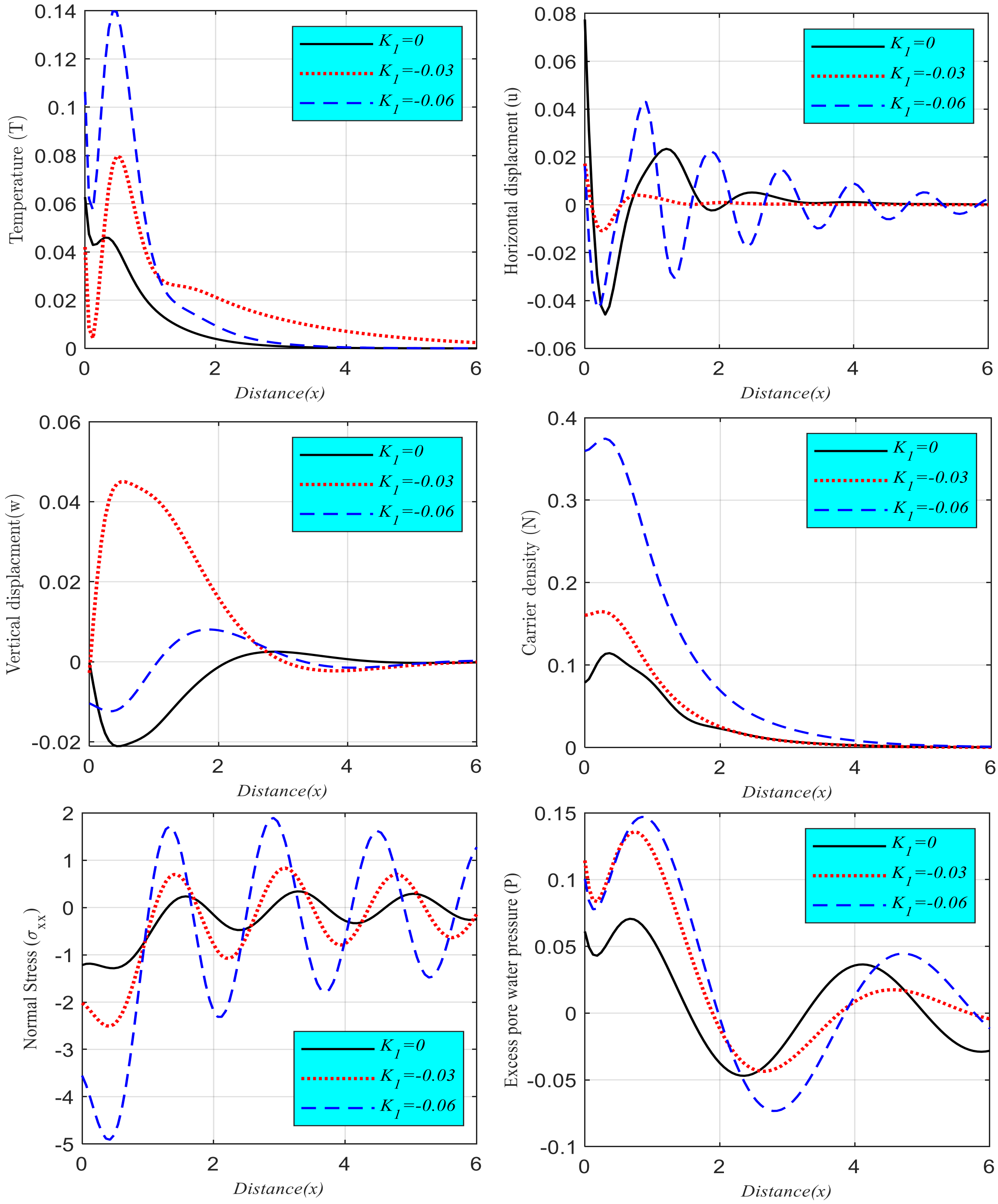

Figure 2. The results of wave propagation of the primary physical fields against distance for different values of variable thermal conductivity are obtained under the effect of the rotational field, decay parameter, and fractional heat order.

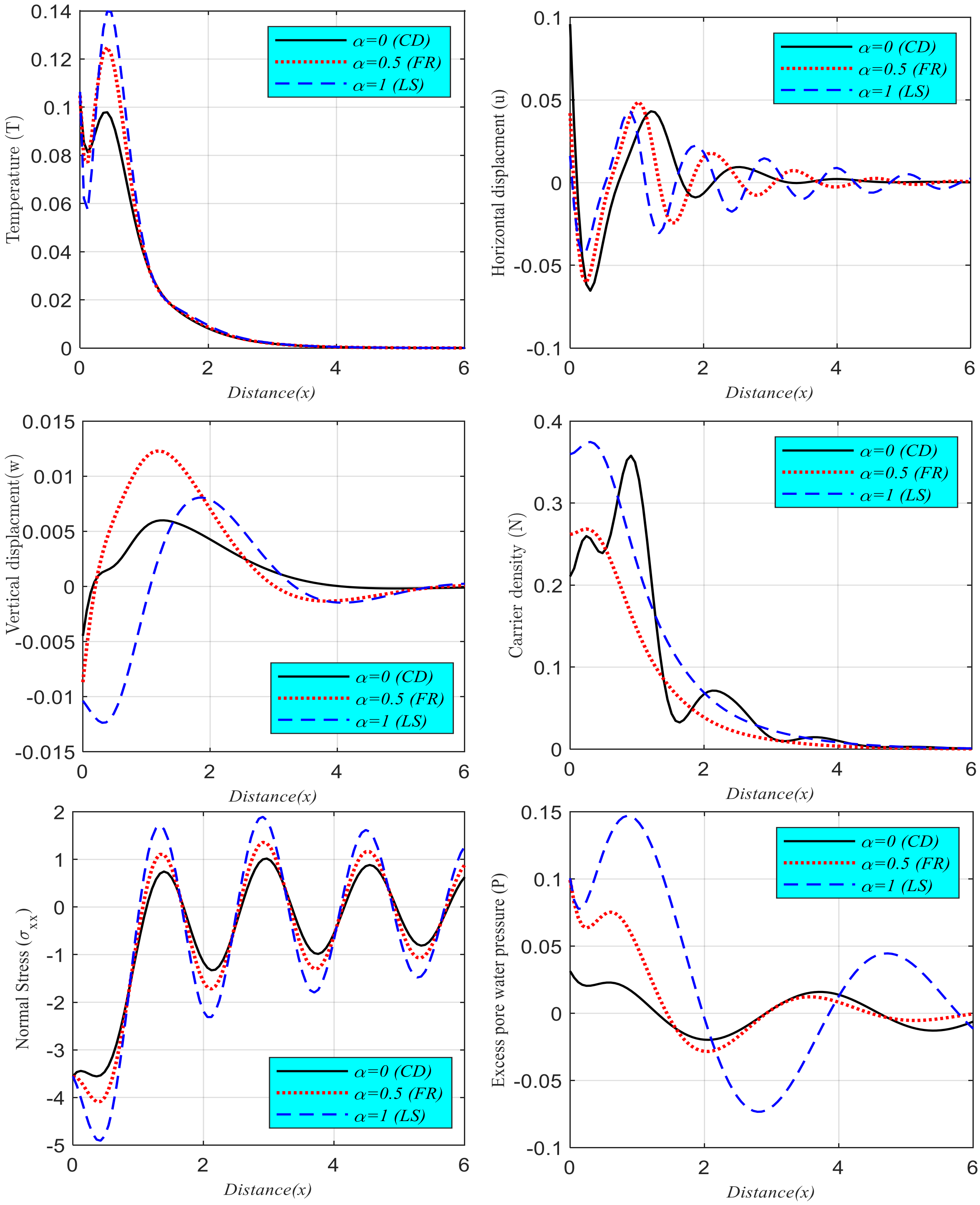

Figure 3. Influence of the fractional-order parameter on the main dimensionless physical fields in a hydro-semiconductor medium subjected to rotational effects and variable thermal conductivity with a decay parameter.

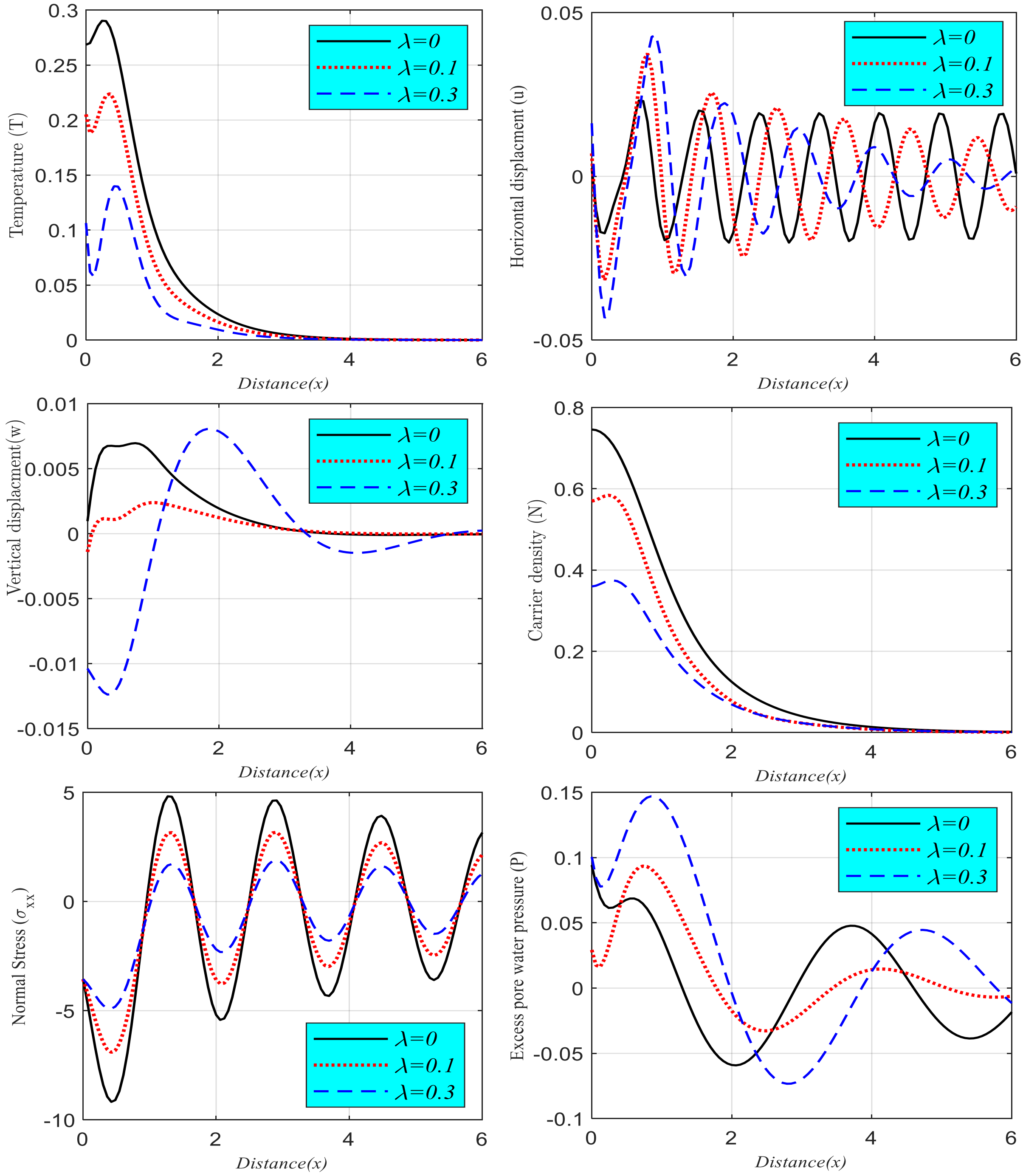

Figure 4. Wave propagation of the primary physical fields against distance for different decay parameter values under the influence of a rotational field, fractional order, and variable thermal conductivity. The computations are carried out to demonstrate the effect of decay parameters on wave oscillatory behavior.